Intermediate closed state for glycine receptor function revealed by cysteine cross-linking

Marie S. Prevost[a,b,c], Gustavo Moraga-Cid[a,b], Catherine Van Renterghem[a,b], Stuart J. Edelstein[d], Jean-Pierre Changeux[e,f,1], and Pierre-Jean Corringer[a,b,1]

[a]Channel Receptors Unit, Institut Pasteur, 75015 Paris, France; [b]Centre National de la Recherche Scientifique, Unité Mixte de Recherche 3571, 75015 Paris, France; [c]Université Pierre et Marie Curie, Cellule Pasteur, 75015 Paris, France; [d]The Babraham Institute, Cambridge CB22 3AT, United Kingdom; [e]Institut Pasteur, 75015 Paris, France; and [f]Collège de France, 75005 Paris, France

Contributed by Jean-Pierre Changeux, September 12, 2013 (sent for review June 15, 2013)

Pentameric ligand-gated ion channels (pLGICs) mediate signal transmission by coupling the binding of extracellular ligands to the opening of their ion channel. Agonist binding elicits activation and desensitization of pLGICs, through several conformational states, that are, thus far, incompletely characterized at the structural level. We previously reported for GLIC, a prokaryotic pLGIC, that cross-linking of a pair of cysteines at both sides of the extracellular and transmembrane domain interface stabilizes a locally closed (LC) X-ray structure. Here, we introduced the homologous pair of cysteines on the human α1 glycine receptor. We show by electrophysiology that cysteine cross-linking produces a gain-of-function phenotype characterized by concomitant constitutive openings, increased agonist potency, and equalization of efficacies of full and partial agonists. However, it also produces a reduction of maximal currents at saturating agonist concentrations without change of the unitary channel conductance, an effect reversed by the positive allosteric modulator propofol. The cross-linking thus favors a unique closed state distinct from the resting and longest-lived desensitized states. Fitting the data according to a three-state allosteric model suggests that it could correspond to a LC conformation. Its plausible assignment to a gating intermediate or a fast-desensitized state is discussed. Overall, our data show that relative movement of two loops at the extracellular-transmembrane interface accompanies orthosteric agonist-mediated gating.

protein conformation | cys-loop receptor | signal transduction

Pentameric ligand-gated ion channels (pLGICs) are major brain receptors mediating signal transduction (1). They transduce agonist binding within their extracellular domain (ECD) into the opening of their ion channel within their transmembrane domain (TMD). This activation process, occurring in the millisecond time range, is followed by slower current decay, corresponding to desensitization processes of channel closing on prolonged agonist application. These events involve the major resting, active, and desensitized states, but also several intermediate states, which correspond to local energy minima within the conformational pathways of the allosteric transitions and are significantly visited during the conformational reorganizations.

In the early 1980s, electrophysiological and rapid mixing binding experiments on nicotinic acetylcholine receptors (nAChRs) demonstrated that desensitization is at least biphasic, with a 10- to 100-ms fast desensitization followed by a 1- to 60-s slow desensitization process (2, 3). Time-resolved affinity labeling showed that the fast- and slow-desensitized states are structurally distinct (4), and electrophysiological recordings suggest that the multiexponential desensitization processes apply to other pLGICs (5). Overall, those data were represented by a minimal four-state (at least) allosteric model in which a central intermediate state accounts for fast desensitization (2, 6–8). In addition, single-channel analysis of desensitization suggest a more complex landscape of more than five short-lived and long-lived conformations that could be distinguished from their kinetic properties (9).

More recently, quantitative characterization by single-channel patch-clamp analysis suggested the occurrence of intermediate steps also in the course of channel activation. A ligand-bound intermediate flip state, stabilized by agonists but carrying a closed channel, was proposed to occur in nAChRs and in glycine receptors (GlyR) (10). Two priming states are required for the fitting of gain-of-function nAChRs mutants (11) and are thought to correspond to a final clamp of the ligand-binding site on binding before channel opening. Finally, Φ-value analysis of hundreds of mutations of the nAChR suggests a conformational wave mechanism where the ECD would move before the TMD during activation (12), pointing an important role of the top of the pore-lining M2 helices and arguing for a multistep process.

Altogether, those results suggest that both activation and desensitization processes are achieved by the transient stabilization of intermediate states to reach the major allosteric conformations. However, the 3D molecular reorganizations underlying these processes remain a challenging issue. Indeed, 3D data about pLGICs mainly concerns prokaryotic pLGICs (1), which have been thus far incompletely characterized at the functional level.

In the course of our study of the proton-gated ion channel Gloeobacter violaceus ligand-gated ion channel (GLIC), a bacterial pLGIC homolog, we solved its X-ray structure in two distinct conformations at supramaximal concentrations of protons (pH 4): an open-channel conformation (13, 14) that is predicted to conduct ions on the basis of molecular dynamic simulations and electrostatic calculations (15), and a locally closed (LC) conformation that is stabilized by disulfide cross-linking at various positions between the ECD and the TMD (16) (Fig. 1). This LC conformation corresponds globally to the open conformation, with a notably quasi-identical outer structure, but

Significance

Glycine receptors are ligand-gated ion channels involved in inhibitory synaptic communication. These membrane proteins undergo conformational transitions between resting, active (with an open channel), and desensitized (closed) states. For the present paper, we chemically cross-linked two regions in the upper part of the ion channel. We show by electrophysiological methods that it results in the stabilization of a new closed state. This new state likely corresponds to an "intermediate conformation" occurring during activation or desensitization, yielding insights into the molecular mechanism of signal transduction.

Author contributions: M.S.P., J.-P.C., and P.-J.C. designed research; M.S.P., G.M.-C., and C.V.R. performed research; M.S.P., G.M.-C., C.V.R., S.J.E., and P.-J.C. analyzed data; and M.S.P., G.M.-C., C.V.R., S.J.E., J.-P.C., and P.-J.C. wrote the paper.

The authors declare no conflict of interest.

Freely available online through the PNAS open access option.

[1]To whom correspondence may be addressed. E-mail: changeux@noos.fr or pjcorrin@pasteur.fr.

This article contains supporting information online at www.pnas.org/lookup/suppl/doi:10.1073/pnas.1317009110/-/DCSupplemental.

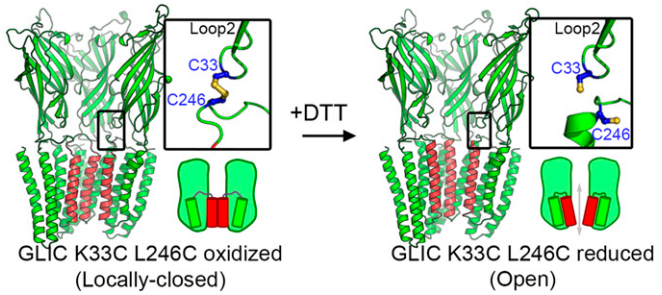

Fig. 1. GLIC-open and GLIC-LC structures. Structure of the cross-linked and reduced forms of the GLIC K33C-L246C mutant. For each form, the pentamer with the two front subunits removed for clarity is seen from the plasma membrane, with the M2 helices colored in red. An enlarged view of the cross-linking region of one subunit is shown for each form with introduced cysteines represented as sticks. A schematic description of each form is drawn beneath the enlarged view.

it carries a closed channel due to a concerted inward bending of the upper part of each of the channel-forming M2 helices (Fig. 1). For every pair of cysteines producing the LC form [between Cys-33 (Loop2) and either Cys-244 (20′), 245 (21′), 246 (22′), or 248 (24′)], DTT reduction before crystallization reestablishes the open form, showing that the disulfide bridge, and not the introduction of cysteines, triggers the LC form (Fig. 1). We further showed that one of the bridges yielding the LC form, the Loop2-22′ GLIC mutant, remains functional by electrophysiology in its cross-linked form, supporting the conclusion that the LC form may exchange with the open form at the membrane and therefore contributes to ligand-gated ion channel function.

To investigate the possible contribution of the LC form to a human and pharmacologically relevant pLGIC, we then constructed the homologous Loop2-22′ mutation on the α1GlyR background (T54C-L274C; Fig. S1), and showed that this cross-linking also preserves the ligand-gated ion channel function in this background (16). In the present paper, we exploit the pharmacology of the α1GlyR and combine whole cell and single channel recordings to analyze in detail the functional consequence of the cross-linking.

Results

Initial Characterization of Single and Double Cysteine Mutants. Mutants were characterized by two-electrode voltage-clamp electrophysiology on expression in *Xenopus* oocytes. As already reported, DTT produces no effect on glycine-evoked currents on the α1GlyR (17). Glycine dose–response curves (Table S1) show that the T54C mutant (EC_{50} = 10 ± 1 μM) exhibits sensitivity to glycine close to that of the WT (EC_{50} = 24 ± 0.2 μM). In contrast, L274C is much less sensitive to glycine (EC_{50} = 1.4 ± 0.06 mM), as already reported for a L274A mutation (18). As expected for an additive effect of the mutations, the T54C-L274C mutant recorded under reducing conditions (after application of 1 mM DTT) displays an EC_{50} of 5.0 ± 0.6 mM (Table S1). Therefore, the L274C mutation in both the WT and T54C context generates a large decrease in sensitivity to glycine. We next investigated the effect of the T54C-L274C cross-linking, which mimics the conditions promoting the LC form in the GLIC crystal.

Multiple Phenotype Caused by the T54C-L274C Cross-Linking. ***Constitutive currents.*** First, under native (i.e., nonreducing) conditions, oocytes injected with the T54C-L274C mutant exhibit a holding current significantly higher than noninjected oocytes (−103 ± 67 nA; Fig. 2 *A* and *B*). This current returns closer to the baseline (−10.6 ± 30 nA) when either DTT (1 mM) or picrotoxin (Fig. S2*A*) are applied to the cell. In contrast, when injected with WT GlyRα1 or single mutants (T54C or L274C), oocytes display resting currents similar to noninjected oocytes. Control experiments monitoring reaction of (2-(trimethylammonium)ethyl methanethiosulfonate) (MTSET) with free cysteines and H_2O_2 oxidation support the conclusion that the T54C-L274C mutant is fully cross-linked in unreduced conditions (Figs. S2*B* and S3). These data show that a disulfide bond is spontaneously formed between the introduced cysteines, which generates constitutive openings of the channel.

Increased glycine sensitivity. Second, dose–response curves show that the unreduced cross-linked form exhibits a 20-fold increase in sensitivity toward glycine compared with the reduced form (EC_{50} = 0.24 ± 0.08 and 5.0 ± 0.6 mM respectively; Fig. 2*B*; Table S1). In addition, activation appears to be slower, and little or no current decay is observed for the cross-linked form (Fig. S2*C*). However, the poor temporal resolution of the oocyte system did not allow us to quantify these differences.

Decreased maximal currents. Third, we found that maximal currents are markedly decreased for the cross-linked form: application of glycine at a near-saturating 10 mM concentration elicits currents that are more than sixfold lower before than after the reduction of the disulfide bond (−0.31 ± 0.2 vs. −1.91 ± 1.0 μA; Fig. 2 *A* and *C*).

Equalization of partial and full agonist efficacy. Fourth, we investigated the action of partial agonists. As observed for the α1GlyR (19, 20), taurine and β-alanine are partial agonists of the reduced T54C-L274C mutant because they elicit, near saturation: 4% and 20% of the glycine maximal response, respectively (Fig. 3). Unexpectedly, the three agonists display the same efficacy (identical response at saturating concentrations) on the cross-linked mutant. As observed for glycine, the cross-linking increases the β-alanine sensitivity (EC_{50} shifted from 19 to 4 mM), whereas the taurine-elicited currents are too small for reliable evaluation of the EC_{50}.

To summarize, compared with its reduced form, the cross-linked T54C-L274C mutant exhibits (*i*) constitutive openings, (*ii*) left-shift of full and partial agonist dose–response curves, (*iii*) decreased maximal glycine-elicited currents, and (*iv*) equalizations of the efficacies of full and partial agonists.

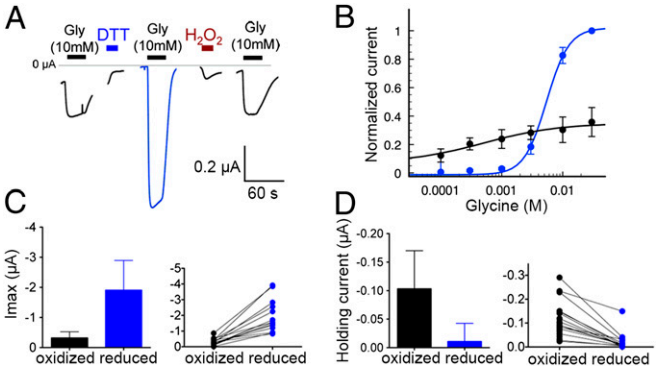

Fig. 2. Spontaneous and glycine-evoked currents of the cross-linked (black) and the reduced (blue) forms of the T54C-L274C GlyR mutant. (*A*) Typical traces of responses to 10 mM glycine and to redox agents of the T54C-L274C GlyR mutant recorded on the same oocyte. For all recordings shown in the present study, a horizontal gray line figures the baseline current, determined as the holding current measured after DTT application. (*B*) Dose–response curves of the glycine receptor current recorded with various concentrations of glycine for the cross-linked (black) and reduced (blue) forms and their fits according to the Hill equation (each point is mean ± SD with $n \geq 3$). Glycine receptor current values are normalized to the value of the 30 mM glycine–evoked current recorded after DTT. (*C*) Maximal glycine-evoked currents recorded before and after 30-s DTT treatment. (*Left*) Bar graph of the maximal holding current as mean ± SD with $n \geq 3$. (*Right*) For each cell, values of the maximal glycine-evoked currents recorded before (black dots) and after DTT (blue dots) are linked by a black line (each point is mean ± SD with $n \geq 3$). (*D*) Spontaneous holding currents before and after DTT treatment, with the same representation as in *C*.

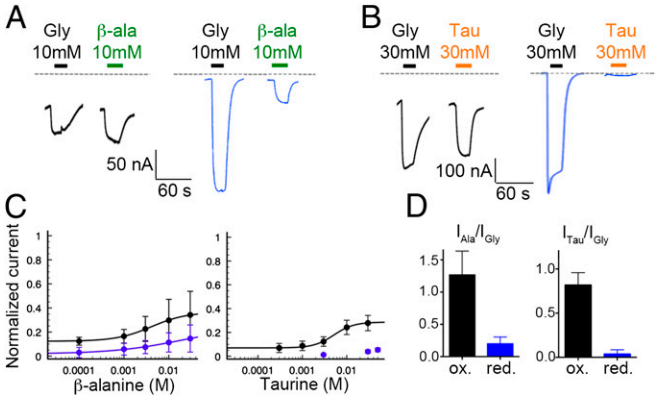

Fig. 3. β-alanine– and taurine-evoked currents of the cross-linked (black) and the reduced (blue) forms of the T54C L274C GlyR mutant. (*A* and *B*) Representative traces of maximal activation by glycine and β-alanine (*A*) or by glycine and taurine (*B*) on the cross-linked (left traces, in black) and reduced (right traces, in blue) forms. All traces in one set (*A* or *B*) were recorded from the same cell. (*C*) Dose–response curves of the glycine receptor current for β-alanine and taurine on the cross-linked (black) and reduced (blue) forms and their fits according to the Hill equation when determinable (each point is mean ± SD with $n \geq 3$). Glycine receptor current normalized to the maximal glycine-evoked current after DTT. (*D*) Ratios between maximal agonist-evoked currents for β-alanine vs. glycine (*Left*) and for taurine vs. glycine (*Right*) for the cross-linked (ox) and reduced (red) forms.

Decrease in Maximal Currents Caused by Cross-Linking Reveals a Unique Closed State. In the context of a minimal two-state Monod-Wyman-Changeux (MWC) model between a resting closed channel R state and an active open channel A state, the occurrence of spontaneous currents implies that the cross-linking strongly stabilizes the A state. According to classical α7nAChR or α1GlyR mutant phenotypes (21), this effect yields an increase in both agonist apparent affinity of activation and efficacy. All effects are observed following the T54C-L274C cross-linking (points 1, 2, and 4), which are therefore well accounted by assuming a simple stabilization of the A state. However, the above gain of function phenotype implies that maximally agonist-elicited currents should be increased, or at least unchanged, on cross-linking. In sharp contrast, we show that the cross-linking markedly decreased the maximal currents by sixfold (point 3).

To test whether this effect is due to a decrease in unitary conductance, we performed patch-clamp recordings of the T54C-L274C mutant after expression in HEK 293 cells. Whole cell recordings gave results qualitatively similar to what is found in oocytes (Fig. 4; Table S2). Before DTT, a significant proportion of receptors are spontaneously open, as revealed by unusually high holding currents (from 50 to 100 pA) inhibited by DTT. Glycine dose–response curves yielded an EC_{50} of 1.2 ± 0.1 mM with maximally evoked currents of 180 ± 80 pA. Reduction with DTT abolished the leak currents, and significantly moved the glycine dose–response curve toward higher concentrations (2.0 ± 0.2 mM), an effect accompanied by a large increase in maximal glycine currents (500 ± 10 pA). We observe no significant difference in the kinetics of activation between the cross-linked and the reduced forms (0.090 ± 0.001 vs. 0.095 ± 0.001 s). However, regarding the current decay after the peak, we found that it is slower when the mutant is cross-linked (27.4 ± 2.6 vs. 0.44 ± 0.1 s; Fig. 4*A*). Single channel recordings show that DTT reduction did not significantly change the unitary conductance of the channel (Fig. 4*D*). Therefore, the increase in maximal currents on reduction is not due to increased single channel conductance.

Thus, at saturating agonist concentrations, cross-linked receptors are not fully activated and remain predominantly in a closed-channel conformation. To further characterize this closed form, we coapplied glycine with the positive allosteric modulators propofol or hexanol on the T54C-L274C expressed in oocytes (Fig. 5 *A* and *B*). We found that propofol potentiates the maximal current elicited by 10 mM glycine on the cross-linked form by 380 ± 180% and 690 ± 410% at 100 and 300 μM, respectively, whereas it has a weak effect on the reduced form. It is likely that higher propofol concentrations, not possible to reach here because of limited solubility, would yield higher potentiation of the cross-linked form. We observe the same pattern of potentiation using hexanol. Interestingly, we also found that when propofol is applied alone, it elicits significant currents on the cross-linked but not the reduced form (Fig. 5*C*). This observation further highlights the gain of function phenotype of the cross-linked form, with the conversion here of a positive allosteric modulator into a partial agonist.

The cross-linking, in addition to producing a gain of function phenotype, thus promotes a unique conformational state, which corresponds to a closed channel conformation that is stabilized by agonists and that is activatable by propofol and hexanol. This state is likely to be neither a slow-desensitized state, because allosteric potentiators cannot activate long-lived desensitized glycine receptors in *Xenopus* oocytes (22), nor the resting state, which is unlikely to be significantly populated at saturating agonist concentration.

Three-State Allosteric Model Fits the Full Cross-Linking Phenotype. The closed state promoted by the T54C-L274C cross-linking thus displays functional properties different from those of states A, R, and D (slow-desensitized). A possible allosteric model would then include a fourth state, named X (Fig. 6 *A* and *B*). To simplify the modeling, we excluded the slow desensitized state in the analysis assuming that, at the steady-state plateau (oxidized form) or at the peak current (reduced form), desensitization is negligible. We thus extended our analysis to an illustrative three-state R-X-A model (Fig. 6; Figs. S4 and S5).

It is noteworthy that the unique closed state is promoted by the same structural constraint that produces the LC form in the GLIC crystal. Assigning a crystal conformation to a functional allosteric state is speculative, but in an attempt to find a possible role for this closed state X, we advance the hypothesis that the conformation adopted by the cross-linked T54C-L274C GlyR mutant in the membrane corresponds to an LC-like conformation. We therefore adjusted the parameters of our three-state R-X-A model so that the X state displays functional properties predicted from the crystal data for the LC conformation (i.e., closed channel and same affinity for the agonist as A, corresponding to the fact that the crystal structure of the ECD is almost the same in the LC and the open conformations).

According to the MWC theory, each state is characterized by an affinity of each of its binding sites for the ligand (site dissociation constants K_R, K_A, K_X), and the system is at equilibrium. $L_{R\text{-}A}$ and $L_{X\text{-}A}$ are the allosteric constants, corresponding to the ratios of the equilibrium concentrations of nonliganded species R_0/A_0 and X_0/A_0, respectively. The electrophysiological response is followed using the function of state $\overline{A}$ [derived from MWC 1965 (23)] that is defined as the proportion of receptors being in the active state, and calculated as

$$\overline{A} = \frac{(1+\alpha)^n}{L_{R\text{-}A}(1+c_{R-A}\alpha)^n + L_{X\text{-}A}(1+c_{X-A}\alpha)^n + (1+\alpha)^n},$$

where α is the ligand concentration divided by its dissociation constant from any site in A (K_A). $c_{R\text{-}A}$ and $c_{X\text{-}A}$ are K_A divided by the dissociation constants from the sites in R (K_R) and in X (K_X), respectively. Finally, n is the number of equivalent and independent binding sites of each receptor, i.e., five for the homopentameric α1GlyR.

With the assumption that X is related to the LC conformation, the nearly identical conformations of the ECDs of the A and X states would imply that $K_A = K_X$ for all agonists. As the cross-linking is located far away from the agonist binding site, we assumed that it does not impair the intrinsic binding affinities but

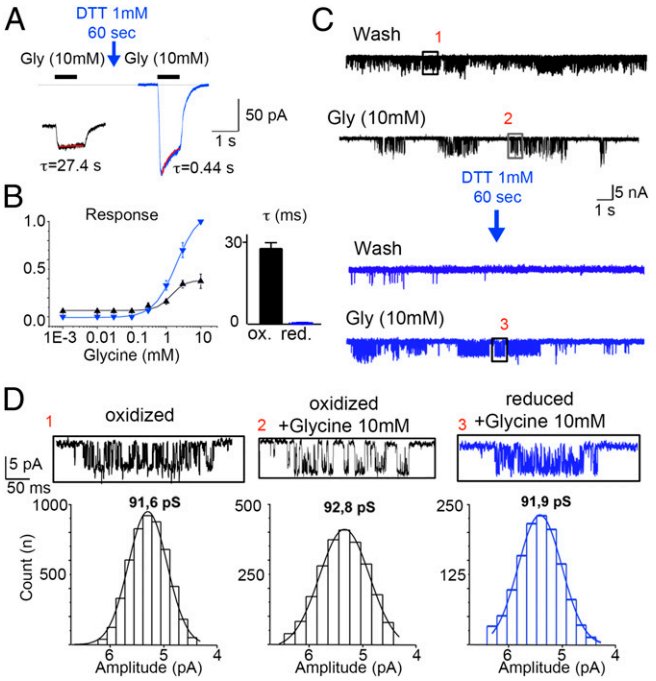

Fig. 4. Whole cell and single channel analysis of the T54C-L274C GlyR mutant in HEK 293 cells. (*A*) Representative traces of spontaneous and glycine-evoked current before and after DTT treatment. Monoexponential fitting of the current decay after peak activation is shown in red. (*B*) Dose–response curves for the glycine-receptor current recorded with glycine before (black) and after (blue) DTT treatment, in the whole cell configuration. Bar graph shows the time constants as calculated in a (mean ± SD with $n \geq 3$). (*C*) Representative single channel recordings for the cross-linked (black) and reduced (blue) forms, in the absence (Wash) or presence (Gly) of glycine. (*D*) Enlargement of boxes shown in *C* and corresponding histograms of current amplitude showing the same unitary conductance in the cross-linked and reduced forms.

only the isomerization constants. Because maximally glycine-elicited currents on the reduced form are weakly potentiated by propofol, we assumed an $\overline{A}$ close to 1 under these conditions. Consequently, the spontaneous currents of the cross-linked form, which are 10-fold weaker, fix $L_{R\text{-}A}$ around 10. Fitting the agonist concentration vs. GlyR current data in both the oxidized and reduced forms then fixes the binding parameters ratios and the allosteric constant $L_{R\text{-}A} = 100$ for the reduced form. Finally, the isomerization constant for the X-to-A transition $L_{X\text{-}A}$ was directly deduced by comparing maximal currents.

The parameters, summarized in Table 1 and Fig. 6*A*, account reasonably well for the entire phenotype (Fig. 6). For the reduced form, given the low representation of the X state due to the low value of $L_{X\text{-}A}$, the $c_{R\text{-}A}$ values allow differentiating between partial ($c_{R\text{-}A} = 0.53$ and 0.63) and full ($c_{R\text{-}A} = 0.22$) agonists. On the cross-linked form, the stabilization of A via the 10-fold change in the $L_{R\text{-}A}$ parameter (that represents a 1.336 kcal/mol gain of free energy compared with R; Fig. S4) leads to the observed spontaneous openings and leftward shifts of the dose–response curves but also accounts for the equalization of efficacies of all types of agonists, because partial agonists are now able to shift the R-A equilibrium far in favor of the A state at saturation. Finally, the stabilization of X ($L_{X\text{-}A} = 2.4$ vs. 0.01, a 4.5 kcal/mol gain of free energy compared with R) accounts for the decrease of maximal currents in the cross-linked form, because at a saturating concentration of glycine, the equilibrium between A and X (30% and 70%, respectively) is predominant.

In conclusion, a three-state model incorporating an X state, with functional characteristics matching those predicted from the LC X-ray structure, reasonably accounts for the present data.

Discussion

Cross-Linking in the Transduction Pathway Reveals a Unique Closed State. In this paper, we cross-linked the ECD and TMD at the level of the M2-M3 loop, which undergoes major structural reorganization concomitant with channel opening/closing within the X-ray structures. At the membrane, such a structural constraint on the M2-M3 loop could limit the relative movement of the TMD and ECD elements and the extent of channel opening. However, we found that the cross-linking does not change the single channel conductance, suggesting that it does not change the structure of the open state. Thus, rather than eliciting a partial gating, it alters the isomerization constants between states. Along this line, we show that the cross-linking stabilizes the active state relative to the resting state and favors a unique closed conformation in the presence of agonist that is likely distinct from both the resting state and slow-desensitized state. Previous work has shown that mutation of loop 2 (24) and loop M2-M3 (18, 25, 26) profoundly altered the glycine receptor function; we show here that relative movement of these two loops at the ECD-TMD interface accompanies orthosteric agonist-mediated gating.

Parallel Structural and Functional Consequences of Cross-Linking Suggest That the Unique Closed State Adopts the LC Conformation. We found that cross-linking that stabilizes an LC conformation of GLIC in the crystal also stabilizes the unique closed state on the α1GlyR. It is noteworthy that GLIC and the α1GlyR share a highly homologous structure despite relatively low (21%) sequence identity: (*i*) the GluCl receptor from *C. elegans*, which shares 34% amino acid identity with the α1GlyR, has an X-ray structure closely related to GLIC with very similar arrangement of loop M2-M3 and loop 2 (27) (0.74-$Å^2$ deviation when the pentamers are superimposed by the α-carbons of those loops), and (*ii*) we constructed a chimera with the ECD of GLIC and the TMD of the α1GlyR and showed that they are functionally compatible to produce a proton-gated chloride channel (28). Thus, the cross-linking should have similar effects on both proteins, suggesting that the unique closed state corresponds to the LC conformation. However, a definite demonstration of this hypothesis would require solving the structure of both the WT and cross-linked mutant of the α1GlyR.

Plausible Functional Contribution of the Unique Closed State to Channel Function. Here, we apply a rather strong structural constraint (cross-linking) on the α1GlyR, which might generate an artificial conformation not adopted by the WT receptors. However, we showed that the equivalent cross-linking on GLIC, as well as three other cross-linking at neighboring positions plus two single mutations, all stabilize the same LC conformation. This evidence suggests that these structural perturbations all stabilize an allosteric state intrinsic to the protein. We may therefore speculate that the unique closed state also applies to the WT glycine receptor, when embedded at the membrane.

According to our allosteric model, the unique closed state, named X, is populated at up to 60% in the cross-linked form at an orthosteric agonist concentration, but this value drops to 5% in the reduced form that is expected to more closely represent what is happening in the WT receptor. However, our modeling only accounts for equilibrium conditions. Weakly populated states may play a key kinetic role, especially if they contribute as intermediates in the gating transition to favor specific pathways. We speculate that X might correspond to an intermediate between resting and active conformations or between active and desensitized conformations.

Concerning the second hypothesis, it is noteworthy that our four-state model R-A-X-D is identical to the R-A-I-D model proposed three decades ago to account for the fast desensitization process. The LC-like conformation would fit well the fast-desensitized motion as evaluated by affinity labeling, which is suggested to involve a large conformational change of the M2 helix compared with the rest of the TMD (4). However, in the

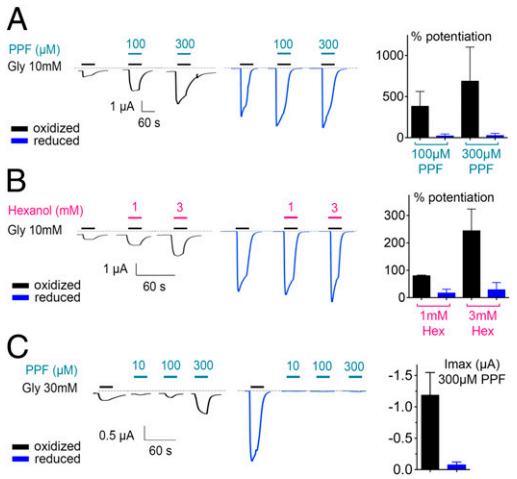

Fig. 5. Propofol modulation of the cross-linked (black) and the reduced (blue) forms of the T54C-L274C GlyR mutant. (*A*) Potentiation of the glycine-evoked currents of the T54C-L274C GlyR mutant by propofol (PPF). (*Left*) Representative trace of the effect of coapplication of glycine and propofol on the oxidized and reduced forms of the mutant recorded on the same cell. (*Right*) Bar graph of the potentiation percentage by propofol at 100 and 300 μM of glycine-evoked currents. (*B*) Potentiation of the glycine-evoked current of the T54C L274C GlyR mutant by hexanol with the same representation as in *A*. (*C*) Direct activation of the T54C L274C GlyR mutant by increasing concentrations of propofol. (*Left*) Representative trace. (*Right*) Values of currents evoked on application of 300 μM of propofol, before and after DTT treatment (mean ± SD, $n \geq 3$).

absence of an identified structure for the longest-lived D state, we cannot speculate about how much the two conformations would differ.

Concerning the first hypothesis, numerous gating intermediates are suggested from the phi analysis on nAChRs (12), with a conformational wave globally from the ECD to the TMD during gating. In this framework, the structure of the LC form would correspond to a fully activated ECD, whereas the TMD would stay closed. This idea would also fit the flip (10) and primed (11) models, which were developed to better fit the single-channel data. The flip conformation displays an affinity higher than the resting state while keeping a shut channel, whereas the primed conformations correspond to progressive capping of the C-loop to trigger several modes of channel opening. The LC form would correspond to a fully capped state. However, it is noteworthy that the above intermediate states correspond to short-lived species (microsecond timescale) that are likely quite unstable, arguing against their trapping by cysteine bridge.

We can further speculate that the LC-like state would serve as an obligatory pivot state to transit between the open state and both closed (resting and desensitized) states, because it is structurally close to that of the open form with an identical overall conformation and orthosteric binding site. In this scheme, the final/initial reorganizations leading to or departing from the open conformation would involve local motions of the pore domain with minor reorganization of the ECD and would thus be independent of the presence and the nature of the ligands acting at the agonist binding site. Interestingly, single-channel experiments provide some data to support this view. Single-channel analysis of the nAChR shows that desensitization rates do not depend on neurotransmitter-binding site occupancy (29). Concerning activation, single-channel analysis of the GlyR suggests that the later step of channel opening, modeled as a transition from the flip to the activated state, is independent of the nature of the bound agonist (10, 30).Overall, the present study does not distinguish between these possibilities but highlights the plausible contribution of an LC-like conformation to the function of human GlyRs.

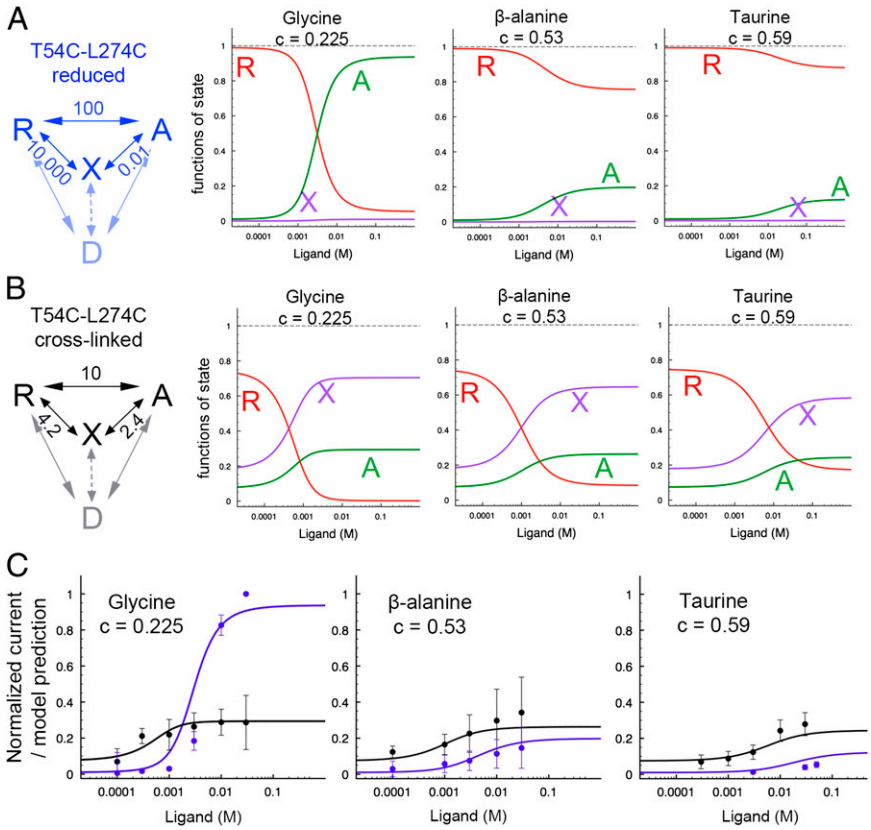

Fig. 6. Modeling of the T54C-L274C GlyR mutant phenotype according to a three-state allosteric model. (*A* and *B*) Allosteric model proposed for the reduced (*A*) and cross-linked (*B*) forms. (*Left*) Scheme of the model: the values of the isomerization constants used in the calculation are given near arrows denoting the state transitions, and the binding of glycine (five sites per pentamer) is not represented for clarity. The transitions to the slow-desensitized state, not included in the present model, are shown in gray tone for illustration. (*Right*) Functions of state of R, A, and X for each agonist for the reduced (*A*) and cross-linked (*B*) forms. (*C*) For each agonist and each form (cross-linked in black, reduced in blue), the function of state Ā is plotted as a solid line superimposed to the experimental data indicated in circles. Data for all agonists are glycine receptor current normalized to the maximal glycine evoked-current on the reduced form (each point is mean ± SD with $n \geq 3$).

Table 1. Parameters used in the proposed model

Receptor	$L_{R\text{-}A}$	$L_{X\text{-}A}$	K_A (glycine)* (M)	K_R (glycine) (M)	K_A^1 (β-alanine) (M)	K_R (β-alanine) (M)	K_A^1 (taurine) (M)	K_R (taurine) (M)
Reduced	100	0.01	9×10^{-4}	4×10^{-3}	1×10^{-3}	2×10^{-3}	5×10^{-3}	8×10^{-3}
Cross-linked	10	2.4	9×10^{-4}	4×10^{-3}	1×10^{-3}	2×10^{-3}	5×10^{-3}	8×10^{-3}

*In the proposed model, we assume $K_A = K_X$ for all agonists.

Conclusion

During the last decade, several X-ray structures of pentameric ligand-gated ion channels have been solved, unraveling a highly conserved architecture among receptor subtypes, but also different conformations where changes in tertiary and quaternary structures are associated with closed and open channels. A key question is now to relate these structures, collected in the artificial environment of the 3D crystal, to allosteric states that contribute to the receptor function at the membrane. In the past, efforts were made to reveal conformational changes undergone by pLGICs using a variety of techniques including electron paramagnetic resonance spectroscopy (31), affinity labeling (4), voltage-clamp fluorometry (20), and cysteine accessibility (17, 32). Those studies confirmed the key role of loops at the interface between the extracellular and transmembrane domains in the gating processes but are subject to ambivalent interpretation at the protein conformation level or in terms of allosteric transitions. In pLGICs, intermediate states during activation and desensitization are often inferred but never directly observed (33) and are poorly characterized at the atomic level. By solving the LC conformation and successfully modeling its occurrence in human pLGICs, we provide the first high-resolution snapshot of a shut allosteric state, distinct from both the resting and desensitized states. This work provides a clue to the understanding of the allosteric pathway at the atomic level and can even be targeted in drug design studies to find new allosteric modulators.

Materials and Methods

Human glycine receptor α1 cDNA inserted in the pmt3 vector was kindly provided by T. Grutter (Strasbourg University, Strasbourg, France) and cysteine mutations were introduced by PCR. Mutant cDNA sequences were confirmed by automated fluorescent DNA sequencing. Two-electrode voltage-clamp electrophysiology in *Xenopus* oocytes was performed as previously described (16). Whole cell and single channel patch clamp electrophysiology on expression in HEK 293 cells was performed as previously described (15). Details are provided in *SI Materials and Methods*.

ACKNOWLEDGMENTS. We thank Marc Delarue and Frederic Poitevin for helpful comments on the manuscript. This work was supported by a grant from the Agence National de la Recherche and the Fondation pour la Recherche Médicale (to G.M.-C.).

1. Corringer P-J, et al. (2012) Structure and pharmacology of pentameric receptor channels: From bacteria to brain. *Structure* 20(6):941–956.
2. Heidmann T, Changeux JP (1980) Interaction of a fluorescent agonist with the membrane-bound acetylcholine receptor from Torpedo marmorata in the millisecond time range: Resolution of an "intermediate" conformational transition and evidence for positive cooperative effects. *Biochem Biophys Res Commun* 97(3):889–896.
3. Sakmann B, Patlak J, Neher E (1980) Single acetylcholine-activated channels show burst-kinetics in presence of desensitizing concentrations of agonist. *Nature* 286(5768):71–73.
4. Yamodo IH, Chiara DC, Cohen JB, Miller KW (2010) Conformational changes in the nicotinic acetylcholine receptor during gating and desensitization. *Biochemistry* 49(1):156–165.
5. Keramidas A, Lynch JW (2013) An outline of desensitization in pentameric ligand-gated ion channel receptors. *Cell Mol Life Sci* 70(7):1241–1253.
6. Heidmann T, Changeux JP (1978) Structural and functional properties of the acetylcholine receptor protein in its purified and membrane-bound states. *Annu Rev Biochem* 47:317–357.
7. Neubig RR, Cohen JB (1980) Permeability control by cholinergic receptors in Torpedo postsynaptic membranes: Agonist dose-response relations measured at second and millisecond times. *Biochemistry* 19(12):2770–2779.
8. Edelstein SJ, Schaad O, Henry E, Bertrand D, Changeux JP (1996) A kinetic mechanism for nicotinic acetylcholine receptors based on multiple allosteric transitions. *Biol Cybern* 75(5):361–379.
9. Elenes S, Auerbach A (2002) Desensitization of diliganded mouse muscle nicotinic acetylcholine receptor channels. *J Physiol* 541(Pt 2):367–383.
10. Lape R, Colquhoun D, Sivilotti LG (2008) On the nature of partial agonism in the nicotinic receptor superfamily. *Nature* 454(7205):722–727.
11. Mukhtasimova N, Lee WY, Wang H-L, Sine SM (2009) Detection and trapping of intermediate states priming nicotinic receptor channel opening. *Nature* 459(7245):451–454.
12. Purohit P, Mitra A, Auerbach A (2007) A stepwise mechanism for acetylcholine receptor channel gating. *Nature* 446(7138):930–933.
13. Bocquet N, et al. (2009) X-ray structure of a pentameric ligand-gated ion channel in an apparently open conformation. *Nature* 457(7225):111–114.
14. Hilf RJC, Dutzler R (2009) Structure of a potentially open state of a proton-activated pentameric ligand-gated ion channel. *Nature* 457(7225):115–118.
15. Sauguet L, et al. (2013) Structural basis for ion permeation mechanism in pentameric ligand-gated ion channels. *EMBO J* 32(5):728–741.
16. Prevost MS, et al. (2012) A locally closed conformation of a bacterial pentameric proton-gated ion channel. *Nat Struct Mol Biol* 19(6):642–649.
17. Lobo IA, Trudell JR, Harris RA (2004) Cross-linking of glycine receptor transmembrane segments two and three alters coupling of ligand binding with channel opening. *J Neurochem* 90(4):962–969.
18. Lynch JW, et al. (1997) Identification of intracellular and extracellular domains mediating signal transduction in the inhibitory glycine receptor chloride channel. *EMBO J* 16(1):110–120.
19. Schmieden V, Betz H (1995) Pharmacology of the inhibitory glycine receptor: Agonist and antagonist actions of amino acids and piperidine carboxylic acid compounds. *Mol Pharmacol* 48(5):919–927.
20. Pless SA, Dibas MI, Lester HA, Lynch JW (2007) Conformational variability of the glycine receptor M2 domain in response to activation by different agonists. *J Biol Chem* 282(49):36057–36067.
21. Galzi JL, Edelstein SJ, Changeux J (1996) The multiple phenotypes of allosteric receptor mutants. *Proc Natl Acad Sci USA* 93(5):1853–1858.
22. Kirson D, Todorovic J, Mihic SJ (2012) Positive allosteric modulators differentially affect full versus partial agonist activation of the glycine receptor. *J Pharmacol Exp Ther* 342(1):61–70.
23. Monod J, Wyman J, Changeux JP (1965) on the nature of allosteric transitions: A plausible model. *J Mol Biol* 12:88–118.
24. Perkins DI, et al. (2009) Loop 2 structure in glycine and GABA(A) receptors plays a key role in determining ethanol sensitivity. *J Biol Chem* 284(40):27304–27314.
25. Lynch JW, Han NL, Haddrill J, Pierce KD, Schofield PR (2001) The surface accessibility of the glycine receptor M2-M3 loop is increased in the channel open state. *J Neurosci* 21(8):2589–2599.
26. Lape R, Plested AJR, Moroni M, Colquhoun D, Sivilotti LG (2012) The α1K276E startle disease mutation reveals multiple intermediate states in the gating of glycine receptors. *J Neurosci* 32(4):1336–1352.
27. Hibbs RE, Gouaux E (2011) Principles of activation and permeation in an anion-selective Cys-loop receptor. *Nature* 474(7349):54–60.
28. Duret G, et al. (2011) Functional prokaryotic-eukaryotic chimera from the pentameric ligand-gated ion channel family. *Proc Natl Acad Sci USA* 108(29):12143–12148.
29. Auerbach A, Akk G (1998) Desensitization of mouse nicotinic acetylcholine receptor channels. A two-gate mechanism. *J Gen Physiol* 112(2):181–197.
30. Burzomato V, Beato M, Groot-Kormelink PJ, Colquhoun D, Sivilotti LG (2004) Single-channel behavior of heteromeric alpha1beta glycine receptors: An attempt to detect a conformational change before the channel opens. *J Neurosci* 24(48):10924–10940.
31. Velisetty P, Chalamalasetti SV, Chakrapani S (2012) Conformational transitions underlying pore opening and desensitization in membrane-embedded GLIC. *J Biol Chem* 287(44):36864–36872.
32. Parikh RB, Bali M, Akabas MH (2011) Structure of the M2 transmembrane segment of GLIC, a prokaryotic Cys loop receptor homologue from Gloeobacter violaceus, probed by substituted cysteine accessibility. *J Biol Chem* 286(16):14098–14109.
33. Colquhoun D, Lape R (2012) Perspectives on: Conformational coupling in ion channels: Allosteric coupling in ligand-gated ion channels. *J Gen Physiol* 140(6):599–612.

Supporting Information

Prevost et al. 10.1073/pnas.1317009110

SI Materials and Methods

α1 Glycine Receptor Mutants. The WT glycine receptors (GlyR) carries seven endogenous cysteines that are unlikely to react with the two that are introduced, because they are distant from the cross-linking region: three are within the ligand binding site (β1 and a disulfide bridge within the C-loop), two form the conserved cysteine bridge within the cys-loop, one is located at the middle of the M3 helix, and the remaining cysteine is carried by the intracellular domain.

***Xenopus laevis* Oocyte Electrophysiology.** The oocytes were obtained from the Centre de Ressources Biologiques-Rennes. Injected oocytes were incubated in Barth's medium (88 mM NaCl, 1 mM KCl, 2.4 mM $NaHCO_3$, 15 mM Hepes, 0.3 mM $NaNO_3$, 0.7 mM $CaCl_2$, 0.8 $MgSO_4$). The electrophysiological buffers contain 100 mM NaCl, 3 mM KCl, 1 mM $CaCl_2$, 1 mM $MgCl_2$, and 10 mM MES (2-N-morpholino)ethane sulfonic acid and are adjusted to pH 7.5 with NaOH. All reagents are from Sigma-Aldrich except (2-(trimethylammonium)ethyl methanethiosulfonate) (MTSET) that is from Anatrace-Affimetrix. Stock solutions were prepared in water or DMSO and were diluted directly in the buffer to the required concentration with pH adjusted to 7.3. Oocytes were recorded as previously described (1). Traces were analyzed by AxoGraph X and Prism or Plot. All currents were measured at −60 mV. All analyses were made on points that are mean ± SD with at least three cells.

For establishment of the dose–response-curves, the maximal currents of the cross-linked form were measured at the plateau, whereas those of the reduced form were measured at the peak current.

HEK 293 Cells Electrophysiology. Glycine-evoked currents were recorded from transfected HEK 293 cells in the whole cell voltage-clamp configuration at room temperature (20–24 °C) at a holding potential of −60 mV. Patch electrodes were pulled from borosilicate glass and filled with (in mM) 120 CsCl, 10 BAPTA, 10 Hepes (pH 7.4), and 4 $MgCl_2$. The external solution contained (in mM) 150 NaCl, 10 KCl, 2.0 $CaCl_2$, 1.0 $MgCl_2$, 10 Hepes (pH 7.4), and 10 glucose. Recordings were performed with a RK-400 patch-clamp amplifier (Bio-Logic) connected to a computer using a Digidata 1400 digitizer and the software pClamp 10 (Axon Instrument) The amplitude of the glycine current was obtained using a manually applied pulse (3–6 s) of different glycine concentrations (0.001–10 mM), using an outlet tube (200 μm inner dimeter) of a custom-designed gravity-fed microperfusion system positioned 50–120 μm of the recorded cell. The concentration–response curves parameters (EC_{50} and Hill coefficients, n_h) were obtained from the curve fits of normalized concentration–response to the equation $I_{gly} = I_{max}$ (gly) $n_h/[(gly)n_h + (EC_{50})n_h]$. The mean maximal current (I_{max}) indicated the average maximal current elicited by a saturating concentration of glycine (1 or 10 mM).

Single-channel recordings in the outside-out configuration were performed using patch pipettes with tip resistances of 7–15 MOhms after fire polishing. Cells were maintained in extracellular medium containing (in mM) 150 NaCl, 5 KCl, 2 $CaCl_2$, 10 Hepes, and 10 glucose, pH 7.4. The intracellular recording solution contained (in mM) 140 CsCl, 2 MgATP, 10 BAPTA, and 10 Hepes, pH 7.3.Cells were voltage clamped at −60 mV, and the signal was then digitized at a sampling frequency of 10–40 kHz. Glycine was applied locally using a gravity-driven, multiway perfusion system.

1. Prevost MS, et al. (2012) A locally closed conformation of a bacterial pentameric proton-gated ion channel. *Nat Struct Mol Biol* 19(6):642–649.

	Loop2	M2M3 loop
GlyRα1	AE**T**TMD	S**L**PKVSYVK
GLIC	DD**K**AET	N**L**PKTPYMT
GlyRβ	QETTMD	ELPKVSYVK
GABAA1	SDHDME	SLPKVAYAT
nAChα7	DEKNQV	IMPATSDSV
ELIC	NTLEQT	ILPRLPYTT
GluClα	DVVNME	QLPPVSYIK

Fig. S1. Sequence alignments of the Loop 2 and the M2M3 loop regions for several pentameric ligand-gated ion channels (pLGICs).

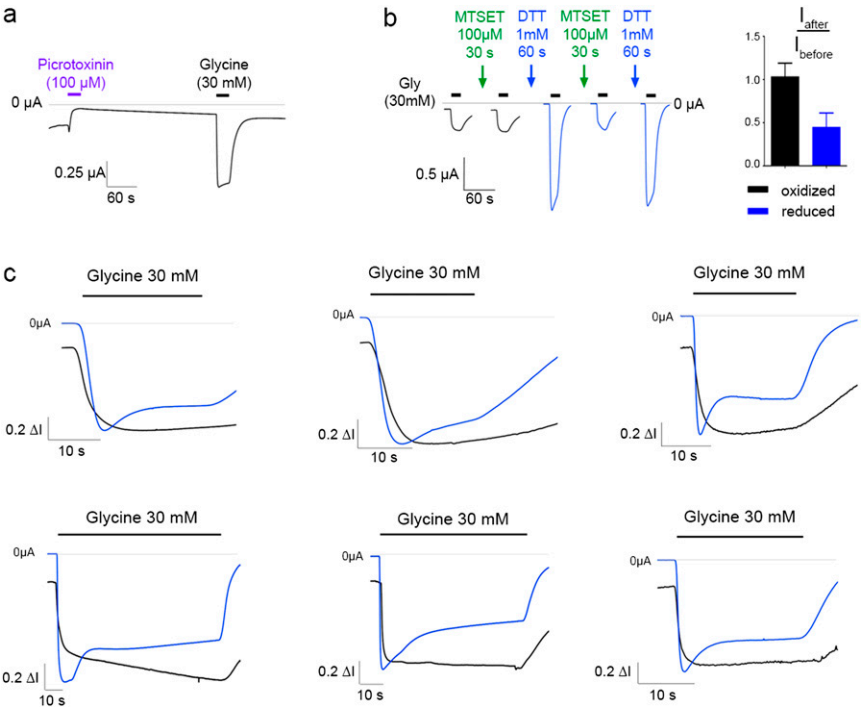

Fig. S2. Properties of the T54C L274C GlyR mutant. (*A*) Representative trace of the effect of picrotoxinin on spontaneous currents of the cross-linked T54C-L274C GlyR mutant. Note that the picrotoxinin block is slowly reversible on washing. (*B*) To evaluate the completeness of the cross-linking in native conditions, we used the free cysteine reagent MTSET. To test whether a proportion of the introduced cysteines display free sulfhydryl groups accessible to cysteine-reactive agents (i.e., not engaged in a disulfide bond), we applied MTSET at 100 μM during 30 s between two saturating glycine pulses, before and after DTT application. A 30-s application of MTSET (100 μM) in native conditions does not modify significantly the maximal glycine-elicited currents. By contrast, after reduction with DTT, MTSET decreases maximal glycine-elicited currents by about 60%, suggesting a predominant, if not complete, cross-linking in native conditions. Note that MTSET does not change the function of WT receptors in an irreversible manner (1). (*Left*) Representative traces obtained on a single cell. (*Right*) Changes in maximal glycine-elicited currents after MTSET treatment for the cross-linked and reduced forms of the T54C-L274C mutant. Bars are mean ± SD for four cells. (*C*) Example of traces highlighting the kinetic differences in the apparent activation, desensitization, and deactivation between the cross-linked (black traces) and the reduced (blue traces) forms of the T54C-L274C GlyR mutant. In each example, the recording was made on a single cell and the applications of glycine had the same duration. Each trace is normalized to its maximum glycine receptor current amplitude to allow visual comparison.

1. Lynch JW, Han NL, Haddrill J, Pierce KD, Schofield PR (2001) The surface accessibility of the glycine receptor M2-M3 loop is increased in the channel open state. *J Neurosci* 21(8): 2589–2599.

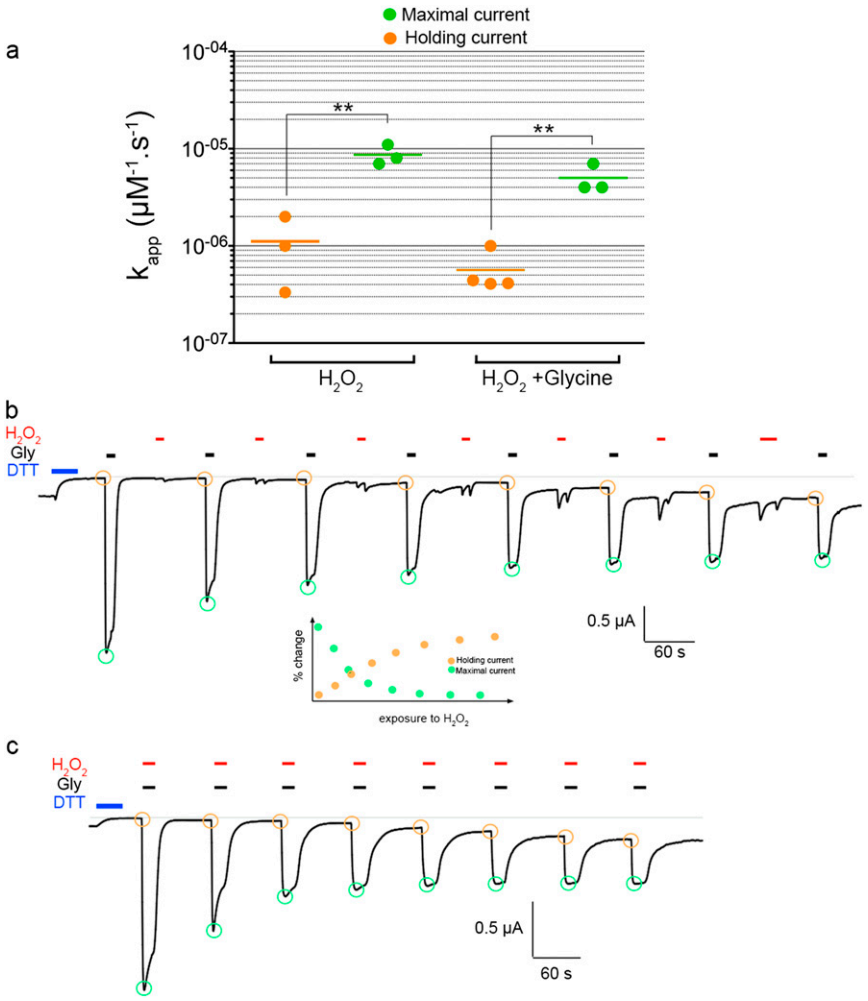

Fig. S3. Kinetics of oxidation of the T54C-L274C GlyR mutant. We submitted oocytes expressing the double-cysteine mutant previously reduced by DTT to oxidation by hydrogen peroxide in a time-resolved manner. After prolonged H_2O_2 application, both the steady-state glycine receptor current in the absence of agonist and the glycine-evoked current have amplitudes similar to those of native currents, further supporting the conclusion that receptors are fully cross-linked in native conditions. (*A*) The kinetic constants were deduced from a single exponential fit of the decrease or increase in current with successive applications of H_2O_2. The constant is evaluated as a function of the total time of exposure to H_2O_2 [i.e., expressed in (µM of H_2O_2 * duration of application in s^{-1}]. The apparent rate constants deduced for the maximal glycine-evoked current (I_{Gly}max) and for the glycine receptor current in the absence of agonist (I_0) were significantly different in an unpaired *t* tested with $P < 0.05$ (**). (*B* and *C*) Examples of traces that allowed the determination of the kinetic constants. The oxidation was monitored by following the increase in spontaneous currents in the absence of agonist, and the decrease in maximal glycine-elicited currents. We found that the decrease in glycine-elicited currents occurs before the increase in spontaneous currents, as revealed by a 10-fold higher first-order kinetic constant. In addition, this effect is independent on the presence of glycine during oxidation. These data suggest that, in the course of the progressive cross-linking of the five cysteine pairs within the pentamer, partial cross linking would be sufficient to promote a reduction in maximal current, and therefore to stabilize the locally closed (LC) conformation, whereas a more complete cross-linking would be required to stabilize the active state over the resting state.

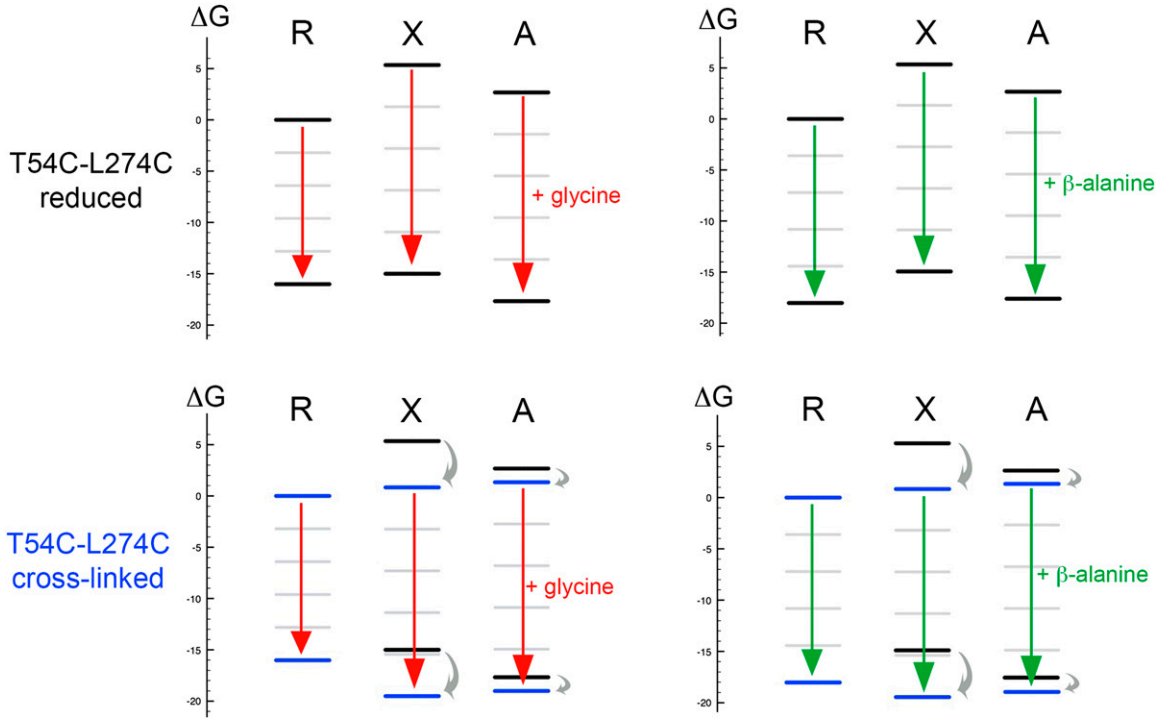

Fig. S4. Free energy diagram of the effect of glycine and β-alanine binding on the three allosteric states, for the reduced (*Upper*) and cross-linked (*Lower*) T54C L274C mutant. All values are normalized to the free energy of R without ligand and are given as kilocalories. Binding of one molecule of glycine or β-alanine generates the same free energy gain for X and A. The cross-linking stabilizes X by 4.5 kcal and A by 1.3 kcal compared with R (at 20 °C).

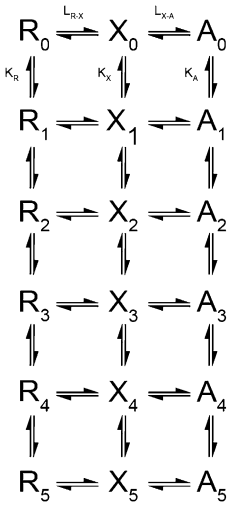

Fig. S5. Three-state allosteric model used to fit the data, where all of the binding steps are explicit.

Table S1. Hill fits of activation by glycine, taurine, and β-alanine in *Xenopus* oocytes

Receptor	nH	EC_{50} (mM)	Imax (μA)	*n*
Reduced (glycine)	2.4 ± 0.4	5.0 ± 0.6	−1.9 ± 1	3
Cross-linked (glycine)	0.69 ± 0.2	0.52 ± 0.2	−0.31 ± 0.2	6
Reduced (β-alanine)	0.56 ± 0.3	19.2 ± 4.0	−0.17 ± 0.1	3
Cross-linked (β-alanine)	1.1 ± 0.1	4.1 ± 0.5	−0.39 ± 0.09	3
Reduced (taurine)	ND	ND	−0.023 ± 0.04	3
Cross-linked (taurine)	1.9 ± 0.5	5.1 ± 1.0	−0.36 ± 0.3	3
T54C (glycine)	1.7 ± 0.6	0.01 ± 0.001	−3.6 ± 0.3	3
L274C (glycine)	1.3 ± 0.08	1.4 ± 0.06	−2.4 ± 0.7	3
WT (glycine)	2.1 ± 0.04	0.024 ± 0.0002	−2.9 ± 1.9	3

ND, not determined.

Table S2. Hill fits of activation by glycine in HEK 293 cells

Receptor	nH	EC_{50} (mM)	Imax (nA)	*n*
Reduced (glycine)	2.1 ± 0.26	2.02 ± 0.2	−0.50 ± 0.1	5
Cross-linked (glycine)	1.3 ± 0.17	1.2 ± 0.1	−0.18 ± 0.08	5
WT (glycine)	2.3 ± 0.24	0.04 ± 0.001	2.9 ± 0.3	5